

Improved net carbon budgets in the US Midwest through direct measured impacts of enhanced weathering

Ilsa B. Kantola^{1,2} | Elena Blanc-Betes³ | Michael D. Masters¹ | Elliot Chang⁴ | Alison Marklein⁴ | Caitlin E. Moore⁵ | Adam von Haden⁶  | Carl J. Bernacchi^{7,8}  | Adam Wolf⁴ | Dimitar Z. Epiphov⁹ | David J. Beerling⁹  | Evan H. DeLucia^{1,2,3,8} 

¹Institute for Sustainability, Energy, and Environment, Carl R. Woese Institute for Genomic Biology, University of Illinois at Urbana-Champaign, Urbana, Illinois, USA

²Carl R. Woese Institute for Genomic Biology, University of Illinois at Urbana-Champaign, Urbana, Illinois, USA

³Center for Applied Bioenergy and Bioproducts Innovation, Institute for Sustainability, Energy, and Environment, University of Illinois at Urbana-Champaign, Urbana, Illinois, USA

⁴Eion Corp., Princeton, New Jersey, USA

⁵School of Agriculture and Environment, The University of Western Australia, Crawley, Western Australia, Australia

⁶Department of Agronomy, University of Wisconsin, Madison, Wisconsin, USA

⁷Global Change Photosynthesis Research Unit, USDA/ARS, Urbana, Illinois, USA

⁸Department of Plant Biology, University of Illinois at Urbana-Champaign, Urbana, Illinois, USA

⁹Department of Animal and Plant Sciences, Leverhulme Centre for Climate Change Mitigation, University of Sheffield, Sheffield, UK

Correspondence

Evan H. DeLucia, Institute for Sustainability, Energy, and Environment, Carl R. Woese Institute for Genomic Biology, Department of Plant Biology, University of Illinois at Urbana-Champaign, Urbana, IL 61801, USA.
 Email: delucia@illinois.edu

Funding information

Leverhulme Trust, Leverhulme Research Centre, Grant/Award Number: RC-2015-029; U.S. Department of Energy, Office of Science, Grant/Award Number: DE-SC0018420

Abstract

Terrestrial enhanced weathering (EW) through the application of Mg- or Ca-rich rock dust to soil is a negative emission technology with the potential to address impacts of climate change. The effectiveness of EW was tested over 4 years by spreading ground basalt ($50 \text{ t ha}^{-1} \text{ year}^{-1}$) on maize/soybean and miscanthus cropping systems in the Midwest US. The major elements of the carbon budget were quantified through measurements of eddy covariance, soil carbon flux, and biomass. The movement of Mg and Ca to deep soil, released by weathering, balanced by a corresponding alkalinity flux, was used to measure the drawdown of CO_2 , where the release of cations from basalt was measured as the ratio of rare earth elements to base cations in the applied rock dust and in the surface soil. Basalt application stimulated peak biomass and net primary production in both cropping systems and caused a small but significant stimulation of soil respiration. Net ecosystem carbon balance (NECB) was strongly negative for maize/soybean (-199 to $-453 \text{ g C m}^{-2} \text{ year}^{-1}$) indicating this system was losing carbon to the atmosphere. Average EW ($102 \text{ g C m}^{-2} \text{ year}^{-1}$) offset carbon loss in the maize/soybean by 23%–42%. NECB of miscanthus was positive (63 – $129 \text{ g C m}^{-2} \text{ year}^{-1}$), indicating carbon gain in the system, and EW greatly increased inorganic carbon storage by an additional $234 \text{ g C m}^{-2} \text{ year}^{-1}$. Our analysis indicates a co-deployment of a perennial biofuel crop (miscanthus) with EW leads to

This is an open access article under the terms of the [Creative Commons Attribution](#) License, which permits use, distribution and reproduction in any medium, provided the original work is properly cited.

© 2023 The Authors. *Global Change Biology* published by John Wiley & Sons Ltd.

major wins—increased harvested yields of 29%–42% with additional carbon dioxide removal (CDR) of 8.6 t CO₂ ha⁻¹ year⁻¹. EW applied to maize/soybean drives a CDR of 3.7 t CO₂ ha⁻¹ year⁻¹, which partially offsets well-established carbon losses from soil from this crop rotation. EW applied in the US Midwest creates measurable improvements to the carbon budgets perennial bioenergy crops and conventional row crops.

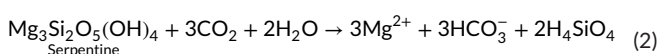
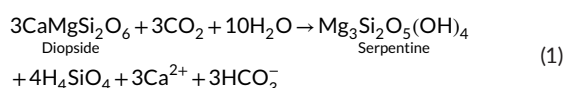
KEY WORDS

agriculture, bioenergy crop, carbon budget, carbon dioxide removal, eddy covariance, enhanced weathering, net ecosystem carbon balance, net primary production, soil respiration

1 | INTRODUCTION

Carbon dioxide removal (CDR) methods are a critical part of climate mitigation strategies (Fargione et al., 2018; Rogelj et al., 2018), and as social and political efforts to reduce carbon emissions to the atmosphere are delayed, the need to implement these strategies earlier in the century is becoming pressing (Hasegawa et al., 2021). Artificially accelerating the natural weathering process of Mg- or Ca-rich rocks, enhanced weathering (EW), can potentially sequester atmospheric carbon (Beerling et al., 2020; Kantola et al., 2017; Kelland et al., 2020; Kohler et al., 2010; Schuiling & Krijgsman, 2006; Taylor et al., 2016), and unlike CDR strategies that build soil organic matter or hold carbon aboveground such as afforestation and reforestation (Minx et al., 2017), most inorganic carbon formed by EW ultimately finds its way to deep ocean deposits where its turnover time is measured in millennia (Hartmann et al., 2013; Renforth & Henderson, 2017), making its storage essentially permanent, at least in the context of climate mitigation.

Over geologic timescales, the weathering of silicate minerals from terrestrial ecosystems and the subsequent deposition of the weathering products as carbonate minerals in oceans plays a key role in controlling atmospheric pCO₂ and stabilizing Earth's climate (Isso et al., 2020; Walker et al., 1981). Natural rock weathering sequesters approximately 0.25 Pg C year⁻¹, or ~3% of fossil fuel emissions (Taylor et al., 2016). This weathering process can be greatly accelerated by the application of ground silicate materials to productive agricultural land, where increased surface area of the material and warm, moist conditions combine to increase the subsequent consumption of CO₂. Ca- and Mg-rich silicate rock powder applied to soil reacts with dissolved CO₂ in the form of carbonic acid to produce bicarbonate (Equations 1 and 2), which eventually is transported in groundwater and runoff to oceans. Weathering reactions that create pedogenic carbonate reduce the amount of CO₂ sequestration but dominant reactions creating bicarbonate represent a potentially large carbon pump from the atmosphere, through terrestrial ecosystems, to the ocean.



In a modeling exercise, the deposition of 40 t ha⁻¹ of ground rock on agricultural lands globally led to net CDR of 0.5–2 Gt CO₂ year⁻¹, comparable to other methods of carbon removal including bioenergy with carbon capture and storage, direct air capture and storage, biochar, soil organic carbon sequestration, and afforestation/reforestation (Beerling et al., 2020). An accounting exercise suggests that CO₂ emissions associated with mining and transportation of rock dust may be fairly small, particularly if the material is sourced from an existing industry (Moosdorf et al., 2014; Renforth, 2018; Renforth et al., 2011), and estimated costs are likely lower than other CDR strategies (Beerling et al., 2020). The efficacy of EW as a CDR strategy, however, requires field tests in various soils and climates.

In a catchment-scale experiment in temperate hardwood forest, part of the Hubbard Brook Experimental Forest was treated with the rapidly weathered Ca-silicate mineral wollastonite in an attempt to reverse severe losses of Ca caused by acid deposition (Taylor et al., 2021). Total annual CO₂ consumption by weathering was calculated as the difference in flow-corrected stream water HCO₃⁻ concentration relative to a control watershed. Even at the relatively low application rate of 3.44 t ha⁻¹ (CaSiO₃), cumulative carbon capture over 15 years was 0.025–0.13 t CO₂ ha⁻¹, with co-benefits of increased wood production and reduced soil respiration from restoring limited Ca and increasing soil pH (Taylor et al., 2021). In contrast, catchment-scale application of 50 t ha⁻¹ year⁻¹ (5 kg m⁻² year⁻¹) basalt to a tropical oil palm plantation in Malaysia for 3 years resulted in no change in alkalinity generation (the measured indicator of CO₂ removal) in two of three catchments (Larkin et al., 2022). Estimates of potential CO₂ removal calculated from the single affected catchment were estimated at 0.4 t CO₂ ha⁻¹ year⁻¹.

In an experiment that did not estimate CO₂ sequestration, greenhouse and garden plot studies performed with wollastonite in food crops with 75 t ha⁻¹ (7.5 kg m⁻²) wollastonite by weight found improvements in growth, yield, and quality of crops produced, as well as increased available Si in the soil (Jariwala et al., 2022). Co-benefits of basalt application were also observed in a mesocosm experiment with the cereal crop, sorghum (*Sorghum bicolor* L. Moench), where the addition of 100 t ha⁻¹ of crushed basalt increased yield by 21% (Kelland et al., 2020). This experiment did not include a direct measure of CDR. However, a model constrained by elemental budgets indicated that CO₂ sequestration rates were 2–4 t CO₂ ha⁻¹ over 5 years, representing a significant increase in carbon capture.

Agricultural landscapes, where the logistics of applying other crushed rock (e.g., limestone) to fields are well established, are attractive systems for EW (Beerling et al., 2020; Kantola et al., 2017). Intensive agriculture associated with row crops—maize (*Zea mays* L.) and soybean [*Glycine max* (L.) Merr.]—is a net source of greenhouse gases, primarily CO₂ and nitrous oxide (N₂O), to the atmosphere (Anderson-Teixeira et al., 2013; Davis et al., 2011), and agriculture, forestry, and land-use change contribute ~24% of global greenhouse gas emissions (US EPA, 2023). In addition to the emission of N₂O associated with fertilizer application and methane (CH₄) from livestock, soil disturbance from aggressive tillage creates a large source of CO₂ to the atmosphere (Verma et al., 2005). EW can potentially reduce emissions of CO₂ from intensive agriculture but, to date, quantification of the efficacy of EW under realistic field conditions is lacking.

Here, we examined the effect of EW on biomass production, the carbon budgets, and rates of inorganic CO₂ removal of a maize/soybean rotation and miscanthus (*Miscanthus × giganteus* Greef et. Deu. ex. Hodkinson et Renvoize) cropping systems under field conditions, on agricultural soils in the Midwestern United States. The maize/soybean rotation is grown on 70Mha in the central US, and miscanthus is an emerging biofuel crop (Davis et al., 2011; Somerville et al., 2010). Miscanthus is a perennial grass with a deep, expansive root system (Anderson-Teixeira et al., 2013; Kantola et al., 2022), attributes that may promote the development of a diverse microbial community in soil which may accelerate the weathering process. Furthermore, we present a direct, measurement-based approach to quantify proxies of alkalinity fluxes and subsequent CDR from basalt application to these crops.

2 | MATERIALS AND METHODS

2.1 | Experimental design

Research was conducted at the University of Illinois Energy Farm (40°3'46" N, 88°11'46" W), south of Urbana, Illinois, between 2016 and 2020, where historic land use was more than 100 years of maize/soybean agriculture. Mean annual temperature is 11°C and mean annual precipitation is 1051mm, evenly distributed throughout the year (Angel, 2010; 1981–2010 average). Soils on the site were moderately well drained Dana silt loam (fine-silty, mixed, superactive, mesic Oxyaeric Argiudolls) with inclusions of poorly drained Flanagan (fine, smectitic, mesic Aquic Argiudolls) and Blackberry (fine-silty, mixed, superactive, mesic, Oxyaeric Argiudolls) silt loams that all belong to the Mollisol soil class (USDA NRCS, 2022).

This experiment utilized a randomized block design with five replicates ($n=5$) each for the maize/soybean rotation and perennial miscanthus. Due to the minimum fetch required for eddy covariance (EC) measurements (Moore et al., 2020), one pair of plots was larger (3.8 ha) than the others (0.7 ha) for each crop and the basalt treatment was applied to the entire plot (Figure S1). Within all of the smaller plots, distinct subplots (10m × 20m) were established and randomly assigned as treatment (basalt added) and control (no basalt). Replicate

material or samples from within each plot or subplot were either bulked or averaged to create a single sample or value for each plot. This experimental design produced $n=5$. The maize plots were managed in a 3-year maize–maize–soybean rotation typical of this region, and the miscanthus plots were managed according to the best-known regional practices (Anderson-Teixeira et al., 2013). These miscanthus plots were established in 2008 and were mature at the time of these measurements. Nitrogen fertilizer was applied each year prior to maize planting as 28% urea ammonium nitrate at 168 and 56 kg N ha⁻¹; granular urea fertilizer was applied to miscanthus; fertilizer was not applied during the soybean year of the rotation.

In November 2016, Blue Ridge basalt, a metamorphosed basalt with a high proportion of medium-weathering silicate minerals (see Lewis et al., 2021 for chemical composition and particle size) was applied to maize/soybean plots at a rate of 50tha⁻¹ (5kgm⁻²) using a conventional lime spreading vehicle and chisel plowed under within 24 h. The rate of application was calculated by the vehicle's onboard computer following a moisture test by the operator. The fields then remained undisturbed until spring cultivation operations in April of 2017. The 2016 miscanthus crop, which remains standing in the field over winter, was harvested in late winter 2017. However, heavy rains in the spring of 2017 prevented basalt spreading equipment from accessing these fields, so no basalt was applied in miscanthus for the 2017 growing season. The Blue Ridge basalt application was repeated in the maize/soybean fields in the fall of 2017, 2018, and 2019 following harvest (four applications). Pre-application soil sampling occurred in 2016, all other measurements were made in the growing season following basalt application (2017–2020). An equal amount of basalt was applied to miscanthus beginning in the spring of 2018 and repeated in 2019 and 2020 following harvest (three applications). Because miscanthus is a perennial crop, the basalt was applied to the surface and not tilled into the soil. Basalt application in maize/soybean occurred in the fall of each year after grain harvest, and in miscanthus followed the spring harvest of the previous year's crop.

2.2 | Ecosystem carbon fluxes

The EC (Baldocchi, 2003) technique was used to measure differences in carbon dioxide (CO₂) flux over time from the 3.8 ha plots of maize/soybean and miscanthus, with and without basalt application. The EC method was administered using flux towers located in the center of each large plot and included the same instrumentation and setup as outlined in Moore et al. (2020). In brief, each tower supported an open path infrared gas analyzer (LI-7500RS; LICOR Biosciences) for atmospheric CO₂ and water vapor concentration and a 3D sonic anemometer (81000RE; RM Young) for wind speed and direction, all recorded at 10Hz. Additional aboveground meteorological and belowground soil measurements were made at 30-min intervals as detailed in Moore et al. (2020). All aboveground instruments initially were installed 2.5m above the land surface, and height was adjusted as each crop grew in the growing season to maintain ~1m of height above the canopy.

The 10Hz flux data were processed to 30-min averages using EddyPro (v6.2.0; LICOR Biosciences) as outlined in Moore et al. (2020). The 30-min flux and meteorological data were then quality assured and quality controlled using the PyFluxPro tool (v1.1.0) developed by Isaac et al. (2017). This processing involved removing spikes and applying a 50% footprint filter, see Moore et al. (2020) for details.

Meteorological data were gap-filled by PyFluxPro using external data sourced from a weather station at the University of Illinois Willard Airport (station ID: 725315-94870, 7.4 km away) and ERA5 data from the European Centre for Medium Range Forecasts. Next, a yearly friction velocity (u^*) threshold for each site was calculated using the moving point test (Papale et al., 2006), and applied to each site to exclude flux data when conditions were not sufficient to support vertical turbulent transport (Table S1). The CO_2 flux data were then gap filled using a self-organizing linear output (SOLO) neural network model along with meteorological variables (Isaac et al., 2017). Lastly, net ecosystem exchange (NEE) was partitioned into ecosystem respiration (R_E) and gross primary productivity (GPP) using the nighttime temperature response function of Lloyd and Taylor (1994) and the SOLO model. All GPP, R_E and NEE data reported are the average from these two models (\pm standard error).

2.3 | Soil carbon fluxes

Instantaneous measurements of soil respiration were made at regular intervals throughout each growing season to assess autotrophic and heterotrophic respiration response to basalt additions. Shallow (installed 5–10 cm below the surface) and deep (installed to 50 cm below the surface) polyvinyl chloride (PVC) collars were installed in each plot, and CO_2 flux was measured using a 20-cm diameter LI-8100-103 soil survey chamber and an LI-8100 portable gas analyzer (LICOR Biosciences). The shallow collars provided a measurement of total soil respiration (R_S) and the deeper collars excluded most plant roots to provide an estimate of heterotrophic respiration (R_H). The difference between R_S and R_H was the autotrophic respiration component (R_A) (Black et al., 2016; Kuzyakov, 2006).

Four collar pairs in the 3.8-ha plots and two collar pairs in each of the 0.7-ha plot treatments were installed to account for spatial variability. Replicate crop/treatment measurements were averaged within a plot. Measurements were made from mid-April to early December, depending on planting and harvest dates. Soil respiration fluxes that were more than five standard deviations outside of the mean for a cropping system within a given date, which accounted for only 0.25% of the total measurements, were taken to be non-representative and thus excluded from further analysis (Nelson et al., 2019).

Multiple regression analyses with stepwise addition of parameters indicated that soil temperature explained 71%–78% of R_S variability across crops and treatments ($p < .05$). Instantaneous measurements of R_S were therefore extrapolated to annual totals by assuming a constant inherent temperature sensitivity (308.56 K^{-1}), and period and treatment specific standardized respiration rate

at reference temperature (Gomez-Casanovas et al., 2013; Lloyd & Taylor, 1994). Annual R_H was estimated observing linearly interpolated contributions to R_S . The error term integrates the propagation of uncertainty of fitted parameters.

2.4 | Plant biomass

Aboveground and belowground biomass was collected at peak growing season maximum (estimated by leaf area index measurements, not shown) for each crop. A randomly placed 0.75 m \times 0.75 m quadrat was used to collect aboveground biomass from two locations in each treatment of the 0.7-ha plots and four locations in each of the 3.8-ha plots. Each location was processed independently and the values within each crop/treatment were averaged. All biomass was separated into leaf, stem, and reproductive tissue fractions prior to drying. Three 30-cm soil cores (5.08-cm diameter \times 30-cm depth) were taken within each sampling quadrant with a slide hammer, soil was pooled and then removed with an elutriator to collect roots and rhizomes for belowground biomass. An additional biometric harvest using the same random sampling scheme was conducted immediately prior to field scale machine harvest to obtain yield data (generally early October for maize and soybean, mid-March for miscanthus). Grain was separated from the rest of the biomass in maize and soybean, while miscanthus yield biomass contained both stem and leaf tissue. All plant tissues were oven dried to constant weight, ground, and analyzed for carbon and nitrogen content using an elemental analyzer (Costech EA 3010 CHNSO Analyzer; Costech Analytical Technologies) with apple leaves and acetanilide (National Institute of Science and Technology) as standards.

2.5 | Statistical analysis of plant biomass and ecosystem fluxes

Interannual variation was used to calculate the standard error of the mean for GPP, NEE, and ecosystem respiration (R_E) collected from EC measurements. For each crop, differences between control plots and basalt plots in biomass and soil respiration were tested using a complete block repeated measures ANOVA with crop, year, and their interaction as fixed factors. Statistical analyses of soil respiration were conducted on instantaneous values (Figure S2; Tables S2–S5). Data were transformed to ensure normality and homogeneity of variances. All statistical tests were conducted with Statgraphics Centurion XVI (Statistical Graphics Corporation).

2.6 | Estimate of CDR by EW

To estimate carbon drawdown in the soil by EW, the net loss of Ca and Mg from surface soils to deeper subsurface soils was quantified (Figure S3). The movement of these base cations is primarily charge-balanced by the transport of bicarbonate ions (HCO_3^-),

formed by combining CO_2 and H_2O (Equation 1); thus, the flux of base cations serves as an alkalinity proxy for carbon sequestration. Importantly, some of the base cations may be charged balanced by other anions such as NO_3^- , which can be estimated by measuring leachate nutrient concentrations. The accumulation of rare earth elements (REEs) in surface soil, and the ratio of REEs to base cations in the rock was used to quantify the addition of Ca and Mg to the soil. Besides transport to the subsurface, other losses of Ca and Mg, including secondary mineral formation, plant uptake, and nitrate weathering were accounted for, providing a direct estimate of CDR as invoked by successful addition and mobilization of base cations into the subsurface.

The accumulation of REEs derived from the applied basalt was quantified in the top 30 cm of soil over the 4 years of this study. REE tracers have been instrumental in studying erosion behavior found in soils (Liu et al., 2004). As the crystal lattice structure of the applied rock degrades during weathering, naturally present REEs in the rock are released (Shibata et al., 2006) and subsequently form strong electrostatic bonds with soil constituents, including organic matter (Tang & Johannesson, 2010), minerals (Xiao et al., 2016), and microbes (Ozaki et al., 2006). These sorbed REEs form stable, immobile complexes with the natural environment under a wide range of geochemical conditions, making them suitable for detection and evaluation in variable field-site conditions. Due to REE immobility in soils (Liang et al., 2010), sampling of topsoil enabled a facile approach in studying the true rock application rate of the Blue Ridge meta-basalt in the field and thus allowed for the quantification of Mg and Ca truly added and incorporated into the soil.

To determine rock application rates of basalt, soils were sampled using a 3.175-cm JMC Backsaver sampling device at a depth of 0–10 cm and 10–30 cm from each plot ($n=5$). Soil was sampled pre-application and after 4 years of rock application for maize/soybean plots and 3 years of rock application in miscanthus plots. Soils were air dried to constant moisture, crushed (Dynacrush DC-5; Custom Laboratory Equipment, Inc.), sieved to 2 mm, and mixed thoroughly to achieve homogeneity. Five independent 0–10 and 10–30 cm samples were chosen from each plot and time point, and mixed thoroughly; homogenized samples for 0–10 cm depth and for 10–30 cm depth regimes were subsequently analyzed using a total fusion inductively coupled plasma-mass spectrometry method (TOT-FUS ICP-MS) for concentrations of all REEs. The resultant data were depth-averaged to assimilate REE concentration data for each of the five plot replicates at the pre- and post-application time points. **Supporting Information** (Appendix S2) has been provided illustrating a worked example of the data processing and CDR computation method.

Upon measuring REE concentrations in pre- and post-application soil samples using TOT-FUS ICP-MS, the change in REE concentrations in the soil were plotted against the REE concentrations determined in the Blue-Ridge meta basalt rock. The resultant plots were fit using linear regression. The regressions were forced through a y-intercept of 0 as a method to apply the physical constraint that at non-detectable changes in soil REE concentrations, no amount

of rock was added to the soil. The regression slope determined between post-application soil REEs and rock REEs was then subtracted by the regression slope determined between pre-application soil REEs and rock REEs (Equation 3). The resultant difference equates to the quantity of accumulated REEs between pre-application baseline and post-application time periods (in units of kg rock kg^{-1} soil). Due to the anomalously high concentration of cerium (Ce) in the rock (Ce is the most abundant metal among the REEs) (Migaszewski & Galuszka, 2015), this light, redox-sensitive REE was not included in the regression analysis.

$$v_{\text{post-application}} - v_{\text{pre-application}} = \text{kg rock applied / kg soil}, \quad (3)$$

where v is the regression slope as obtained from plotting soil REE concentrations versus rock REE concentrations.

The calculated slope difference (kg rock kg^{-1} soil) was converted to kg rock m^{-3} units by using estimates of the soil bulk density. This was determined by measuring the mass of dried soil samples contained in tractor-mounted hydraulic soil core samples (cylinder of 1.905 cm radius and 10 cm length for 0–10 cm depth samples and 20 cm length for 10–30 cm depth samples; Giddings Machine Company). Bulk density measurements (144 total) from 0 to 10 cm and 10 to 30 cm depth were averaged, and the average bulk density (Kantola et al., 2023) was used to calculate the mass of rock per unit volume (kg m^{-3}). The total sampling depth of 30 cm was used to ultimately convert the rock application rate units to kg rock m^{-2} units.

Uncertainty associated with the regression slope determination was estimated using a least squares regression method. Uncertainty was further propagated in converting the initial uncertainty value (kg rock kg^{-1} soil) to kg rock m^{-2} units.

The increase in soil pH (6.2–6.8 between 2017 and 2020 for maize at 0–10 cm depth, 5.6–6.0 in miscanthus; I. B. Kantola, unpublished) with the addition of Blue-Ridge meta basalt may also result in the formation of amorphous Al(OH)_3 , SiO_2 , or Fe(OH)_3 secondary mineral phases (Lewis et al., 2021), which may indirectly reduce the translocation of weathering products (Mg, Ca base cations) due to increased sorption and exchange sites. To account for the precipitation of these alternate phases, post-application soil samples were analyzed for Mg and Ca concentrations using a TOT-FUS ICP-MS method. Specifically, post-application soil samples were analyzed to determine the persistent Mg and Ca cations ($[\text{Mg}]_{\text{surficial processes}}$, $[\text{Ca}]_{\text{surficial processes}}$) that have not left the top 30 cm boundary condition (Equations 4 and 5). This measurement addresses the cumulative reduction in aqueous Mg and Ca ions as a result of surficial geochemical processes, such as secondary mineral formation and creation of additional sorption sites (Lewis et al., 2021), ion-exchange (Levy, 1980), and interlayer clay interactions (Kumari & Mohan, 2021).

The concentration of Ca and Mg taken up by maize, soybean (D. Z. Epihov, unpublished), and miscanthus potentially reduces the aqueous alkalinating potential of the base cations released from basalt dissolution. For maize and soybean plots, the concentration of base cations measured in root samples were summed with base cation concentrations measured in the shoot

samples using inductively coupled plasma-optical emission spectroscopy (ICP-OES) methods. The concentration of base cations multiplied by peak biomass (leaves and stems, 2017–2020) was used to estimate the total uptake of base cations for each crop ($[Ca]_{\text{plant uptake}}$ and $[Mg]_{\text{plant uptake}}$). For the miscanthus plot, biomass from leaves, stems, floral material, roots and rhizomes were collected for each year (2018–2020) and analyzed using ICP-OES methods to quantify plant uptake of Ca and Mg cations. Total biomass of aboveground plant parts were calculated for 2018–2020 (Table S6). Belowground plant parts (root and rhizome) were estimated using root:shoot and rhizome:shoot ratios, following Dohleman et al. (2012).

To assess nitrate and ammonia loss through leaching, resin lysimeters (ion-exchange resin beads packed in PVC and nylon mesh to allow water infiltration) were buried at 50 cm below the surface in each plot, extracted after 1 year and replaced annually throughout the duration of the experiment. The ion exchange resin was carefully removed, shaken with 2 M KCl for 1 h in a reciprocal shaker, and filtered through a Whatman GF/F 0.7 µm filter. The solution was then analyzed for nitrate and ammonia concentrations using colorimetric flow injection analysis (Lachat QuikChem 8000). To provide a conservative CDR estimate, all measured losses of N between the amended and control plots were assumed to be a result of nitrate-based strong acid weathering and subsequent leaching with the aqueous base cations (rock weathering and transport of base cations with NO_3^- instead of with HCO_3^- anions). Specifically, inorganic nitrogen concentrations were summed across all years (2017–2020 for maize/soybean and 2018–2020 for miscanthus plots) for both control and basalt-amended plots. For each crop system, the difference of cumulative collected inorganic nitrogen concentration was determined between control and basalt-amended plots. Conservatively assuming all N is NO_3^- , this difference (reported in kg N ha^{-1}) was converted to a mol $N \text{ m}^{-2}$ quantity (Alkalinity_{nitrate loss}), allowing for an equivalence subtraction of nitrate-based strong acid leaching from the total alkalinity pool obtained from Mg/Ca release into the soil, where 2 moles of nitrate pair with each mole of either Mg or Ca.

Multiple direct soil-based measurements have been described to determine true rock application rate, base cation losses associated with secondary mineral formation and other subsurface geochemical processes, and plant uptake of base cations. The aforementioned quantities were synthesized using the following equations (Equations 4 and 5) to determine total Mg and Ca concentrations that result in soil alkalinity increases:

$$[Mg]_{\text{rock application}} - [Mg]_{\text{surficial processes}} - [Mg]_{\text{plant uptake}} = \text{Net Mg Gain}, \quad (4)$$

$$[Ca]_{\text{rock application}} - [Ca]_{\text{surficial processes}} - [Ca]_{\text{plant uptake}} = \text{Net Ca Gain}, \quad (5)$$

where [Mg] and [Ca] are quantified for processes of rock application, surficial (loss) processes, and plant uptake. Units of net gain are represented in mol base cation m^{-2} .

The increase in base cation concentrations, accounting for alkalinity loss from nitrate strong acid leaching, was then converted to a CDR potential as in the following equation:

$$(\text{CO}_2\text{-factor} \times (\text{Net Mg Gain} + \text{Net Ca Gain}) - \text{Alkalinity}_{\text{nitrato loss}}) \times \text{M.W.CO}_2 = \text{CDR}, \quad (6)$$

where net gain of base cations (in mol m^{-2} units) are converted to permanent alkalinity stored in the ocean by a CO_2 -factor that incorporates the fact that some CO_2 is released during riverine transport and ocean storage (1.6 mol CO_2 mol⁻¹ cation, Renforth & Henderson, 2017) and the molecular weight of CO_2 (M.W. CO_2 , 44.01 g mol⁻¹). Alkalinity loss associated with strong acid/nitrate leaching is also addressed (mol nitratem⁻²). All nitrate was conservatively assumed to charge-balance divalent base cations using a 1:2 stoichiometry (i.e., 2 moles of nitrate inhibit 1 mole of Mg from leaching).

2.7 | Carbon budget

The biomass and flux data for each crop were used to assemble a partial carbon budget where the input into the system is represented by GPP and combined losses are represented by ecosystem respiration (R_E) as in Chapin et al. (2006). GPP, NEE, and R_E were partitioned from the eddy flux data as described previously. Harvest represents material removed from each plot either as grain for maize and soybean (I. B. Kantola, unpublished) or total aboveground biomass for miscanthus. Net ecosystem carbon balance (NECB) was calculated as NEE minus harvest and represents residual carbon in the ecosystem available for conversion to soil organic carbon. Net primary production (NPP) was calculated as the sum of annual above- and belowground biomass increments. For the annual crops, maize and soybean, harvested biomass (above- and belowground) was used for this calculation. For the perennial crop, miscanthus, peak biomass was used as the aboveground biomass increment. Belowground NPP was calculated as the sum of rhizome and fine root NPP, where rhizome NPP was calculated as peak rhizome biomass multiplied by a turnover rate of 0.2 year⁻¹ (Wildova et al., 2007) and fine root NPP was calculated as peak root biomass multiplied by a turnover rate of 0.5 year⁻¹ (Gill & Jackson, 2000). The soybean year (2019) was treated independently from the maize carbon budget, and 2017 was omitted from the miscanthus C budget as basalt was not applied that year.

The major pools and fluxes in the carbon budgets were expressed as units of grams carbon (g C m^{-2}), calculated by multiplying the values of dry biomass by the fractional carbon content (0.41–0.46 depending on crop and tissue) or by multiplying fluxes of CO_2 by 12/44. Where the measured variables used to calculate a component of the carbon cycle were different statistically, the overall value for the control plots and plus basalt plots are shown individually (averages for 3 years); a single 3-year average value (maize and miscanthus, single year for soybean) is shown for carbon cycle components where a statistically defensible difference could not be resolved between the measured variables used in their calculation. Because of difficulty

propagating error, statistical analyses were not performed on the carbon cycle values.

3 | RESULTS AND DISCUSSION

3.1 | Carbon fluxes and biomass accumulation

Eddy covariance measurements of NEE and corresponding calculations of GPP and R_E did not resolve differences in organic carbon storage (NEE, NECB) between control plots and basalt-treated plots miscanthus, maize, or soybean (Figure 1). Beginning in mid-May, soon after maize was planted, NEE began to decrease, becoming strongly negative (CO_2 consumption by the crop) as the plant canopy and photosynthesis (GPP) increased during the summer (Figure 1d,e). Annually integrated NEE was higher for basalt-treated maize in one year (2020) but lower in two others (2017, 2018; Tables S2 and S3) and because the instantaneous values overlapped during the year (Figure 1d), integrated average NEE for the control and basalt plots, $(-403 \pm 69$ and $-325 \pm 51 \text{ g C m}^{-2} \text{ year}^{-1}$, respectively, Table S2) were not considered different. The values of maize NEE during the years of the basalt treatment (2017–2020) were considerably more negative, indicating a stronger potential carbon sink,

than pretreatment data collected from the same plot in 2009–2015 ($69 \pm 106 \text{ g C m}^{-2} \text{ year}^{-1}$, Table S3). During this time, maize was a net source of CO_2 to the atmosphere. Central Illinois experienced unusually high temperatures and a severe drought during the summer of 2012 (Joo et al., 2016) and the legacy of this drought, manifested as a combination of lower GPP and higher R_E reduced the average historic values (2009–2015) for NEE (Bernacchi et al., 2022; Blakely et al., 2022; Moore et al., 2022). Consistent with Verma et al. (2005) and Suyker and Verma (2012) the smaller stature soybean (Figure 2) had lower GPP than maize or miscanthus (Figure 1; Tables S2 and S4). Soybean typically had positive NEE (Table S4) indicating that like maize it was a net source of CO_2 to the atmosphere.

As with maize and soybean, no difference in integrated NEE could be resolved between basalt treated ($-759 \pm 52 \text{ g C m}^{-2} \text{ year}^{-1}$, Tables S2 and S5) and control plots ($-655 \pm 71 \text{ g C m}^{-2} \text{ year}^{-1}$) of miscanthus (Figure 1d). NEE was, however, considerably greater for miscanthus than maize and soybean, and this difference was driven primarily by lower R_E in miscanthus (Figure 1c,f) and its longer effective growing season. As a perennial crop, the emergence of miscanthus early in the growing season, the development of greater total leaf area, and the presence of a functional canopy later in the growing season enables it to achieve greater seasonally integrated photosynthesis than maize (Figure 1a,d), even

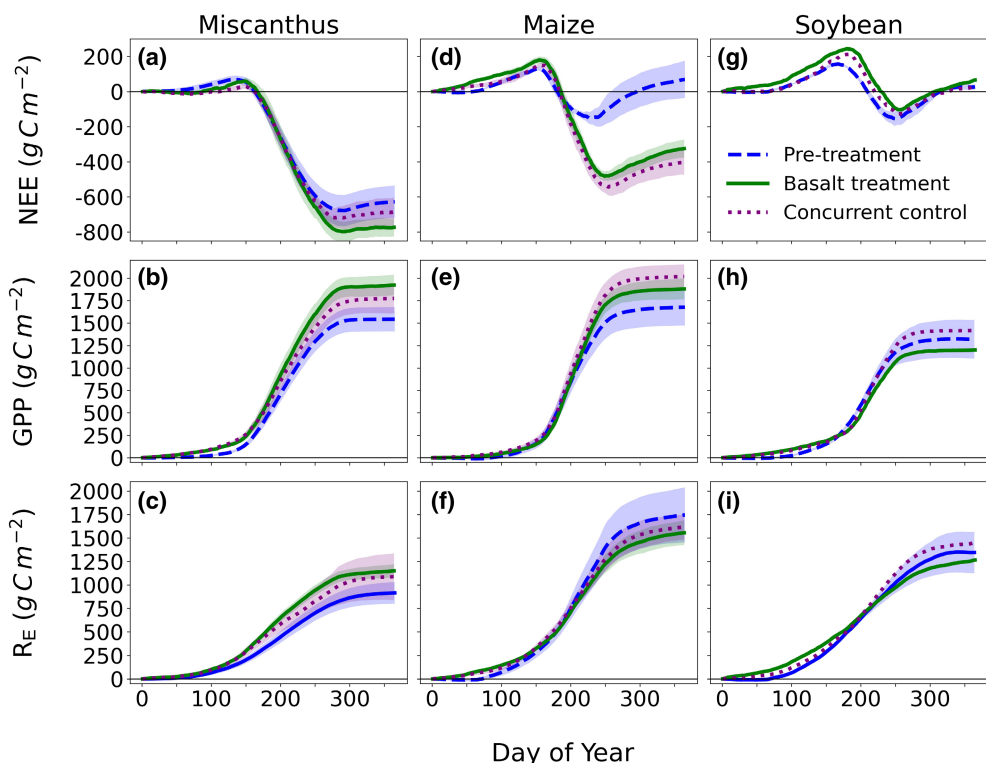


FIGURE 1 Mean annual cumulative net ecosystem exchange (NEE), gross primary productivity (GPP) and ecosystem respiration (R_E) for miscanthus (a–c), maize (d–f) and soybean (g–i), respectively, measured by eddy covariance. Measurements were made at the University of Illinois Energy Farm, Illinois, United States from 2009 to 2020. For maize, pre-treatment years include 2009, 2011, 2012, 2014, 2015, and basalt treatment and concurrent control years include 2017, 2018, 2020. For miscanthus, pre-treatment years include 2009–2017, and basalt treatment and concurrent control years include 2018–2020. For soybean, pretreatment years include 2010, 2013, 2016, and basalt treatment and concurrent control occurred in 2019. The shading around the mean cumulative curve represents the standard error of the mean, which also demonstrates inter-annual variability in the fluxes.

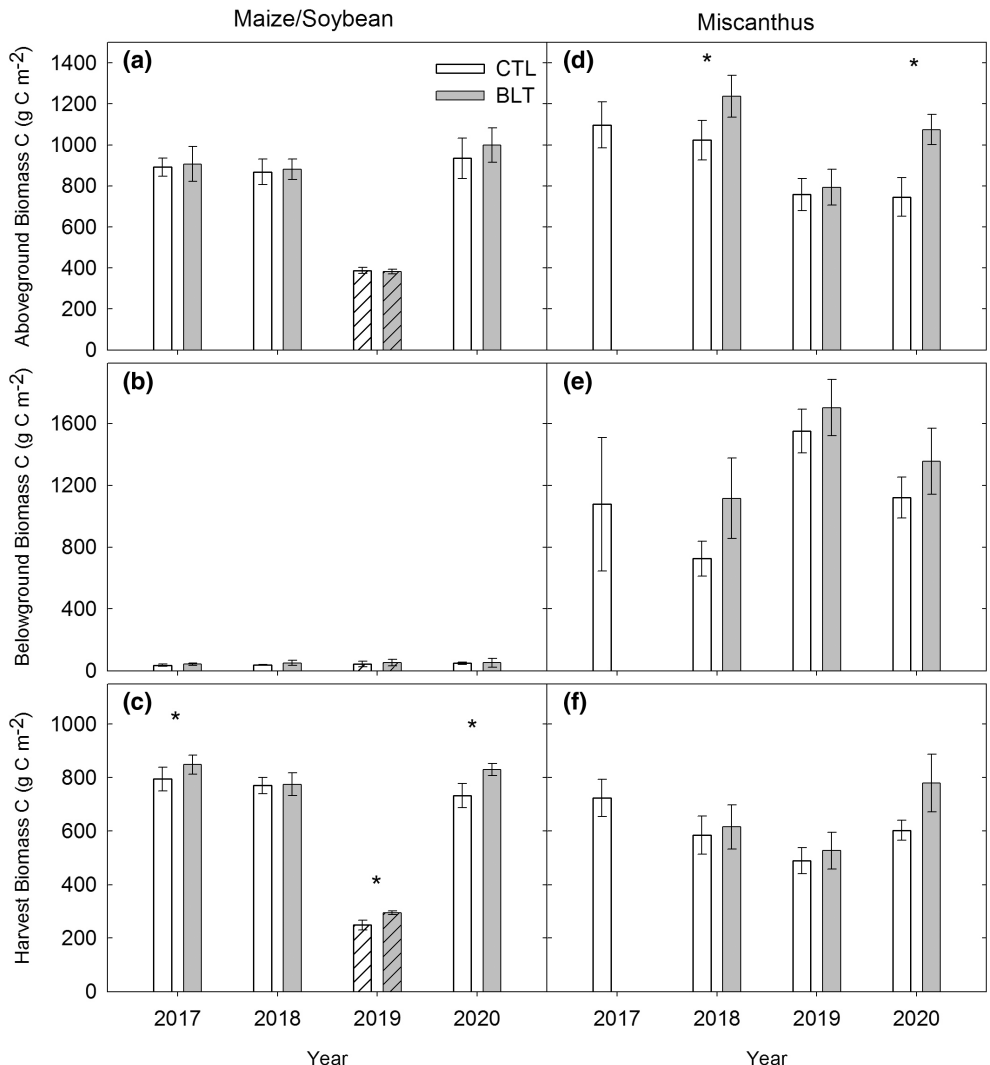


FIGURE 2 Peak above- and belowground biomass and harvested biomass for maize, soybean (hatched bars), and miscanthus grown in control plots (open bars) or plots treated with basalt (shaded bars). Aboveground, belowground, and harvested biomass for maize and soybean are shown in (a, b, and c), respectively; and, aboveground, belowground and harvested biomass for miscanthus are shown in (d, e, and f), respectively. Peak sampling time was determined by weekly leaf area index measurements (not shown). Belowground biomass for miscanthus included roots plus rhizomes. Bars represent mean values \pm one standard error. Asterisks indicate statistically significant differences ($p < .05$). There were no statistically significant differences in peak maize or soybean biomass for plants grown under control or plus basalt treatments, however, harvested biomass was greater for maize under the basalt treatment. Aboveground miscanthus biomass (2018 and 2020) and belowground biomass (2018) was significantly greater for plants grown with basalt than control plants. Because of bad weather, basalt was not applied to miscanthus plots 2017.

though maize has higher instantaneous rates of leaf photosynthesis (Dohleman & Long, 2009). Miscanthus maintained high rates of evapotranspiration through the 2012 drought by mining deep soil water reserves (Joo et al., 2017) and biomass yield remained suppressed for several years without the addition of nitrogen fertilizer (Kantola et al., 2022).

Basalt treatment did not affect above- or belowground peak biomass carbon for maize or soybean (Figure 2; Table S6), but increased grain biomass carbon and grain yield by 12% (2020) and 16% (2019) for maize and soybean, respectively (D. J. Beerling, D. Z. Epihov, I. B. Kantola, M. D. Masters, T. Reeshemius, N. J. Planavsky, C. T. Reinhard, J. Jordan, S. J. Thorne, J. Webber, M. Val Martin, S. E.

Hartley, C. Larkin, R. James, C. Pearce, E. H. DeLucia, S. A. Banwart, unpublished; Kantola et al., 2023). Peak biomass represents the maximum carbon acquired by the plant during the growing season, and occurs prior to grain setting in maize. In recent years, average corn and soybean yields in Illinois have been steadily increasing. Since the region-wide drought in 2012, the state of Illinois has seen a period of higher than predicted yields in maize, likely due to a combination of technological improvements and favorable weather conditions (Schnitkey et al., 2021). This trend will continue for the near term, however, sensitivity to increased temperature and atmospheric vapor pressure deficit will likely limit yields in the future (DeLucia et al., 2019; Lobell et al., 2014).

Maize is intensively fertilized in the American Midwest, often to the detriment of nearby bodies of water. High rates of nitrogen fertilizer application results in the gradual acidification of soils, which limits N uptake by plants (Anda et al., 2015; Gillman et al., 2002). Acidification is managed by intermittent liming of maize fields; however, the control plots in this experiment have received no lime since 2012. The application of basalt to these soils has a liming effect (Blanc-Betes et al., 2020; D. J. Beerling, D. Z. Epiphov, I. B. Kantola, M. D. Masters, T. Reeshemius, N. J. Planavsky, C. T. Reinhard, J. Jordan, S. J. Thorne, J. Webber, M. Val Martin, S. E. Hartley, C. Larkin, R. James, C. Pearce, E. H. DeLucia, S. A. Banwart, unpublished), which may alter the behavior of the soil microbial community, increase nitrogen use efficiency (NUE), and result in changes in availability of plant essential nutrients. Modeling results and measurements in these plots indicate increased NUE in basalt-treated maize and miscanthus (D. J. Beerling, D. Z. Epiphov, I. B. Kantola, M. D. Masters, T. Reeshemius, N. J. Planavsky, C. T. Reinhard, J. Jordan, S. J. Thorne, J. Webber, M. Val Martin, S. E. Hartley, C. Larkin, R. James, C. Pearce, E. H. DeLucia, S. A. Banwart, unpublished), which may account for the increase in yield (Figure 2c; Blanc-Betes et al., 2020). Additionally, Blue Ridge basalt is 0.09% P (Lewis et al., 2021), supplying a small amount of plant-essential P to the system. Best management practices for maize production in the Midwest require additions of P and K every few years to maintain yields, however, to not confound measurements of basalt weathering, these fields have not received P and K since 2014. Model predictions for this site show the combination of P addition and soil pH increases by basalt addition to positively affect annual productivity and grain yield in maize (Blanc-Betes et al., 2020).

In contrast with maize, basalt application stimulated peak aboveground biomass carbon accumulation in miscanthus by 29% and 42% in 2018 and 2020, respectively (Figure 2d; Table S6), without significant effects on harvest yields. Because miscanthus was harvested in late winter/early spring, several months later than estimates of peak biomass, loss of senesced leaves caused harvested biomass to be substantially lower than peak biomass, masking the effect of basalt on yield.

As previously stated, basalt application has a liming effect that may enhance N uptake by miscanthus, potentially increasing plant growth. Miscanthus on this site receives 56 kg N ha^{-1} annually to support yields, however, like maize, the miscanthus fields were un-limed during this experiment (previous liming occurred prior to miscanthus establishment in 2008). Miscanthus re-translocates nutrients to the root system at the end of the growing season for use the following year which reduces the need for nutrient addition (Davis et al., 2010; Hudiburg et al., 2014); miscanthus plots have not received P or K fertilizer since establishment. While model results do not predict a yield enhancement of miscanthus with basalt addition (Blanc-Betes et al., 2020), P provided by basalt weathering may support the observed increase in peak biomass in this study. D. J. Beerling, D. Z. Epiphov, I. B. Kantola, M. D. Masters, T. Reeshemius, N. J. Planavsky, C. T. Reinhard, J. Jordan, S. J. Thorne, J. Webber, M. Val Martin, S. E. Hartley, C. Larkin, R. James, C. Pearce, E. H. DeLucia, S.

A. Banwart (unpublished data) observed higher transcript levels for genes associated with nutrient mineralization and uptake for roots of soybean and maize treated with basalt, supporting the hypothesis its application enhances nutrient availability.

At peak biomass, the difference in carbon allocation of these species was striking, with miscanthus allocating 28x more biomass belowground than maize (Figure 2b,e; Kantola et al., 2022). The large investment in belowground biomass by miscanthus greatly increases the potential for belowground organic carbon storage for this species (Anderson-Teixeira et al., 2009, 2013; Kantola et al., 2022), further increasing the climate benefits of growing this emerging bioenergy crop beyond displacing fossil fuels. Additionally, the greater root biomass of miscanthus increases the potential for basalt weathering by root-associated organic acids and phytosiderophores exuded by miscanthus roots (Chen et al., 2018), and larger belowground inputs could positively affect microbial communities in the miscanthus rhizosphere. This is further evidenced by concomitantly greater heterotrophic and autotrophic soil respiration relative to maize/soybean.

Soil respiration (R_S) was generally higher in basalt treated maize and soybean than in controls, though only measurements for 2017 and 2019 were statistically significant ($p < .05$; Figure 3; Tables S7 and S8). This is consistent with positive effects of high pH on soil organic carbon availability to soil microorganisms (Curtin et al., 1998). Measurements of soil microbial biomass further supported this view by showing greater soil microbial biomass in basalt-treated soil than control soil (Figure S4). Furthermore, the relative abundance of predatory bacteria (typically correlating with greater number of soil bacteria i.e., prey) was also significantly higher in basalt-treated soil communities. The partitioning of soil respiration between heterotrophic (R_H) and autotrophic (R_A) respiration was not consistent between years, with higher R_H observed in basalt-treated maize in 2018, and lower R_H in 2017, 2019, and 2020 (Tables S7 and S8). In miscanthus, basalt application resulted in significantly higher R_S in 2019 and 2020, driven by significantly higher R_H in those years (Tables S7 and S9). At least in the control plots, the ratio of R_A/R_H was generally greater in miscanthus than the row crops likely due to lack of soil disturbance from tillage and greater belowground biomass for the perennial crop (Anderson-Teixeira et al., 2013; Kantola et al., 2022). The overall changes in R_S were small in both crops, indicating that the effect of basalt on the soil microbiome had little impact on respiration directly, and observed differences can likely be attributed to secondary effects on biomass or interannual variability.

3.2 | CDR by EW

The measured accumulation of immobilized REEs (Figure S5) present in the maize/soybean topsoil yielded an estimate of basalt application of $20.2 \pm 1.4\text{ kg m}^{-2}$ (Figure 4a), which is consistent with the *a priori* value of 20 kg m^{-2} (four treatments of 5 kg m^{-2} , or 50 tha^{-1}) applied between the fall of 2016 and the 2020 growing season. Basalt treatment on maize-soybean fields resulted in a potential carbon

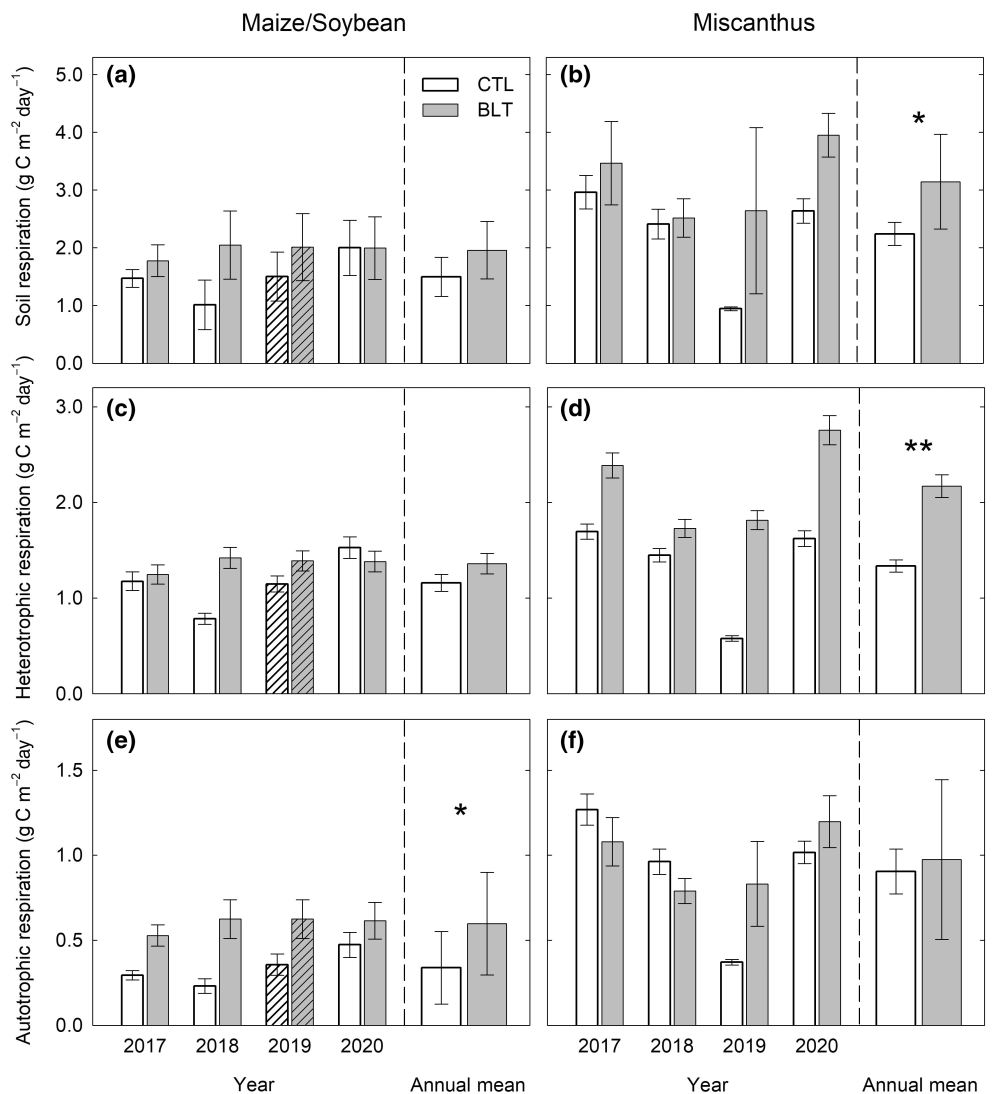


FIGURE 3 Average daily soil respiration over the course of a year was calculated by gap filling instantaneous values (Figure S2) for maize, soybean (a, c, and e), and miscanthus (b, d, and f). Bars represent mean values \pm one standard error. Open bars represent control and shaded bars represent basalt addition. Total soil respiration and heterotrophic soil respiration were measured directly and autotrophic (root) soil respiration was calculated by subtracting heterotrophic respiration from total soil respiration. Statistical analyses conducted on instantaneous values (Tables S6 and S7) revealed that both R_s and R_h were significantly greater in miscanthus than maize; these components of R_s also were significantly greater for basalt amended plots than controls (Tables S8 and S9). Asterisks indicate statistically significant differences (Tables S8 and S9) of instantaneous values (Figure S2). Data for maize and soybean were combined for statistical analyses because of low number of measurements for soybean.

removal estimate of $102 \pm 4.9 \text{ g C m}^{-2} \text{ year}^{-1}$. Within the CDR budget associated with rock weathering, 1.8% of the alkalinity flux was conservatively estimated as weathered and leached with nitrate while 4.5% was absorbed via plant uptake and utilization mechanisms (Figure 4c). Based on elemental mass balance, the remaining 93.7% of the alkalinity flux entered the deeper soil subsurface. An alternate CDR quantification technique using titanium isotope dilution mass spectrometry on the same field study yielded a comparable CDR estimate of $130 \pm 75 \text{ g C m}^{-2} \text{ year}^{-1}$ (D. J. Beerling, D. Z. Epihov, I. B. Kantola, M. D. Masters, T. Reeshemius, N. J. Planavsky, C. T. Reinhard, J. Jordan, S. J. Thorne, J. Webber, M. Val Martin, S. E. Hartley, C. Larkin, R. James, C. Pearce, E. H. DeLucia, S. A. Banwart,

unpublished data), corroborating the CDR value reported in this study using REEs as tracers. The cumulative CDR normalized by rock application rate was estimated as $18.42 \text{ kg CO}_2 \text{ t}^{-1} \text{ rock year}^{-1}$ between 2016 and 2020, comparable to calibrated reactive transport models from Vienne et al. (2022) that report $17.92 \text{ kg CO}_2 \text{ t}^{-1} \text{ rock year}^{-1}$ across a 5-year simulation.

Because miscanthus fields were not tilled after initial planting, surface soil properties were likely more variable and less homogenized with time than maize-soy soils exposed to mechanical disturbance. This potential enhanced variability in soil texture and geochemistry resulted in a different suite of optimal lanthanides to be used for application rate determination (Figure S5). Light REEs (La

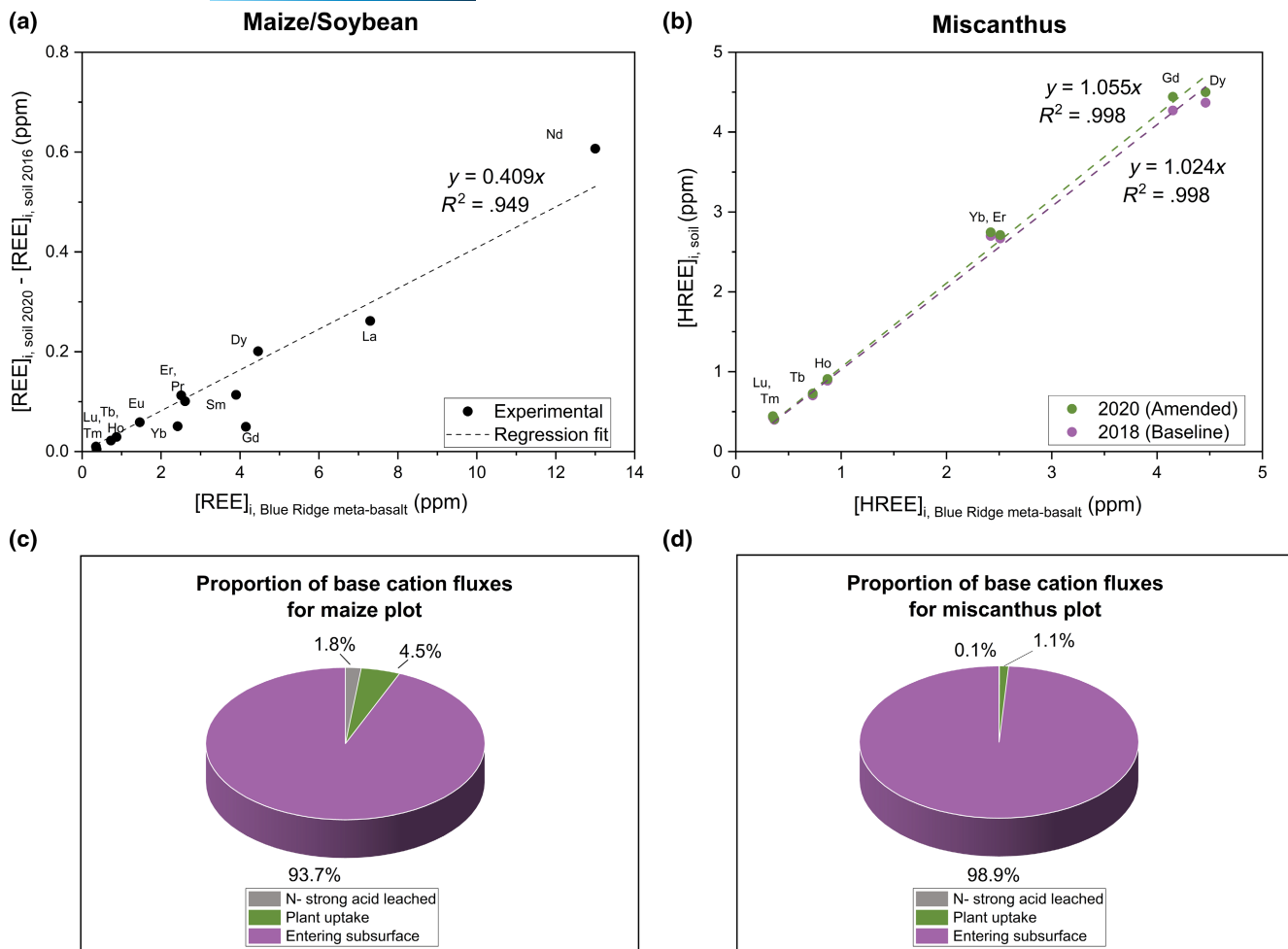


FIGURE 4 Cumulative rock addition was determined through direct measurement of (a) the change in total soil REE concentrations between 2016 and 2020 on maize/soybean plots, and (b) the change in total soil heavy REE concentrations between 2018 and 2020 on miscanthus plots. The change in heavy REE concentration in soils as represented in (b) was more clearly illustrated as two regressions (pre- and post-applied lines), though the difference of the two regression slopes yields a single sloped line as demonstrated by (a) under the use of the full REE suite. The proportion of base cation fluxes entering the deeper subsurface soils was quantified for (c) maize-soybean plots and (d) miscanthus plots through soil, lysimeter, and plant tissue measurements. REE, rare earth element.

to Gd) have been shown to adsorb weaker to solid-phase ligands than heavy REEs (Tb to Lu) (Chang et al., 2021; Takahashi et al., 2014). Furthermore, the rock REE signal-to-soil background noise ratio is greater for heavy REEs (ratio >1) in contrast with the signal-to-noise ratio for light REEs (ratio <1). As such, the regression of heavy REE change in the soil between pre- and post-application times was used in the miscanthus system, yielding a very high correlation ($R^2 = .998$). An estimated rock application rate of $14.5 \pm 1.6 \text{ kg m}^{-2}$ (Figure 4b) was reported, consistent with the a priori value of 15 kg m^{-2} (three applications of 50 t ha^{-1} or 5 kg m^{-2}) applied between 2018 and 2020. The miscanthus system yielded a potential carbon removal estimate of $234 \pm 18.3 \text{ g C m}^{-2} \text{ year}^{-1}$. Within the CDR budget, 0.1% of base cation transport was conservatively estimated to leach with nitrate, 1.1% was lost via plant uptake, and 98.9% was estimated to have leached into the subsurface (Figure 4d). Notably, 69% of the Mg and 64% of the Ca that was applied to the miscanthus plots leached into deeper subsurface soils, while only 29% of Mg and Ca added in the

maize-soybean system left the top 30 cm soil boundary condition. This can be explained by the deeper root and more prolific root system for miscanthus than maize (Black et al., 2017), as well as the greater plant respiration estimates for miscanthus than maize, suggesting higher partial pressures of subsurface CO_2 that could stimulate rock weathering and subsequent leaching of base cations. An example set of calculations for the maize/soybean plots have been made available in Appendix S2.

Annual basalt application of 50 t ha^{-1} (5 kg m^{-2}) as presented in this study has the potential to sequester $8.6 \text{ t CO}_2 \text{ ha}^{-1} \text{ year}^{-1}$ in miscanthus fields and $3.7 \text{ t CO}_2 \text{ ha}^{-1} \text{ year}^{-1}$ in maize/soybean fields. The CDR estimate for EW applied to miscanthus plots under relatively high application rates of basalt show promise in comparison with other nature-based negative emission technology solutions (Table 1). California rangeland amended with 0.25 inches of compost yielded a $7.7 \text{ t CO}_2 \text{ ha}^{-1} \text{ year}^{-1}$ CDR potential (Silver et al., 2018) and annual biochar application at 2.5 t ha^{-1} sequestered $6.7 \text{ t CO}_2 \text{ ha}^{-1} \text{ year}^{-1}$

TABLE 1 Comparison of CDR potentials for nature-based NET solutions.

Treatment	Carbon dioxide removal potential ($t\text{CO}_2\text{ha}^{-1}\text{year}^{-1}$)	SE ($t\text{CO}_2\text{ha}^{-1}\text{year}^{-1}$)	Carbon form	Annual application rate (tha^{-1})
Basalt EW on miscanthus plots ^a	8.6	0.65	Inorganic	50
Compost amendment ^b	7.7		Organic	6.4
Biochar application ^c	6.7		Organic	2.5
Basalt EW on maize/soybean plots ^a	3.7	0.18	Inorganic	50
Deep soil inversion ^d	3.6		Organic	Not applicable

Note: Values for carbon dioxide removal potential are averages plus or minus the standard error of the mean (SE).

Abbreviations: CDR, carbon dioxide removal; EW, enhanced weathering; NET, negative emissions technology; SE, standard error.

^aThis study.

^bSilver et al. (2018).

^cFawzy et al. (2022).

^dAlcántara et al. (2016).

(Fawzy et al., 2022). Deep soil plowing led to a $3.6\text{tCO}_2\text{ha}^{-1}$ increase in organic carbon stock (Alcántara et al., 2016). Of the observed nature-based solutions, a large application of Blue Ridge basalt in productive US Midwest soils grown with miscanthus poses the highest carbon removal potential with the additional benefit of sequestering an inorganic form of carbon. We note that CDR efficiency ($\text{tCO}_2\text{t}^{-1}$ material) may vary for each of these technologies as a function of application rate and frequency ($\text{t material ha}^{-1}\text{year}^{-1}$), as well as soil type, climate, and dominant crop. The clear relationship between crop NPP and observed weathering rates, both greatest in the miscanthus crop, would be indicative of greater potential for weathering in the generally more productive maize than soybean (Figure 5). However, soybean reveals similar weathering effects to those generated by maize (D. J. Beerling, D. Z. Epihov, I. B. Kantola, M. D. Masters, T. Reeshemius, N. J. Planavsky, C. T. Reinhard, J. Jordan, S. J. Thorne, J. Webber, M. Val Martin, S. E. Hartley, C. Larkin, R. James, C. Pearce, E. H. DeLucia, S. A. Banwart, unpublished data). These findings support the utility of N_2 -fixing crops to trigger substantial weathering rates with lower environmental and economic tradeoffs (no N application), as previously recorded (Epihov et al., 2017, 2021).

3.3 | Carbon budget for maize/soybean and miscanthus cropping systems

Eddy covariance values, hand-sampled biomass, and field measurements of soil respiration were combined to develop a partial carbon (C) budget for the maize/soybean and miscanthus cropping systems under EW treatment conditions. Because different methods (EC towers, hand biomass sampling, and survey measurements of soil respiration) were used to measure the components of the carbon budgets, with their own associated uncertainties, the budgets do not balance and should be viewed as approximations.

Carbon inputs, measured as GPP, were broadly similar between the maize years of the maize/soybean rotation and miscanthus (Figure 5). Consistent with Joo et al. (2016) and Moore et al. (2020), higher R_E resulted in lower NPP in maize than in miscanthus. Without basalt, annual estimates of microbial respiration from soil (R_H) in control plots were greater in the maize/soybean rotation (71%–75% of total soil respiration, R_S) than miscanthus (60% of R_S ; Figure 5). Basalt addition stimulated both root respiration (R_A) and microbial respiration (R_H) in miscanthus, corresponding to a consistent but not significant increase miscanthus belowground biomass with basalt (Figure 2).

Net ecosystem carbon balance was calculated as the difference between NEE and harvested biomass (Anderson-Teixeira et al., 2013; Chapin et al., 2006; Joo et al., 2016), and represents carbon remaining in the ecosystem. In these agroecosystem composed of non-woody plants, presumably this carbon is stored in the soil. NECB was negative for maize and soybean indicating that these cropping systems were mining old soil carbon and returning it to the atmosphere (Joo et al., 2016; Zeri et al., 2011). Because basalt increased grain yields for these crops (I. B. Kantola, unpublished data), NECB was more negative under this treatment. Historically in the American Midwest, the conversion of grassland to cropland and particularly maize production have been a net source of carbon to the atmosphere (Anderson-Teixeira et al., 2013; Zhang et al., 2021), and management practices and intensive harvest resulted in soil carbon loss over time. In contrast with the maize/soybean cropping system, miscanthus had positive NECB, naturally sequestering carbon from the time of establishment (2008). During the period between 2018 and 2020, the annual rate of carbon storage in the soil by the miscanthus system averaged $707\text{gCm}^{-2}\text{year}^{-1}$. The large root system (Figure 2) and absence of tillage contributed to accumulation of carbon in miscanthus (Anderson-Teixeira et al., 2009, 2013).

In both cropping systems, carbon uptake and transport to ground water as HCO_3^- by EW was substantial. EW of $102\text{gCm}^{-2}\text{year}^{-1}$ mitigated carbon losses from the maize/soybean cropping system by

(a) Maize/Soybean

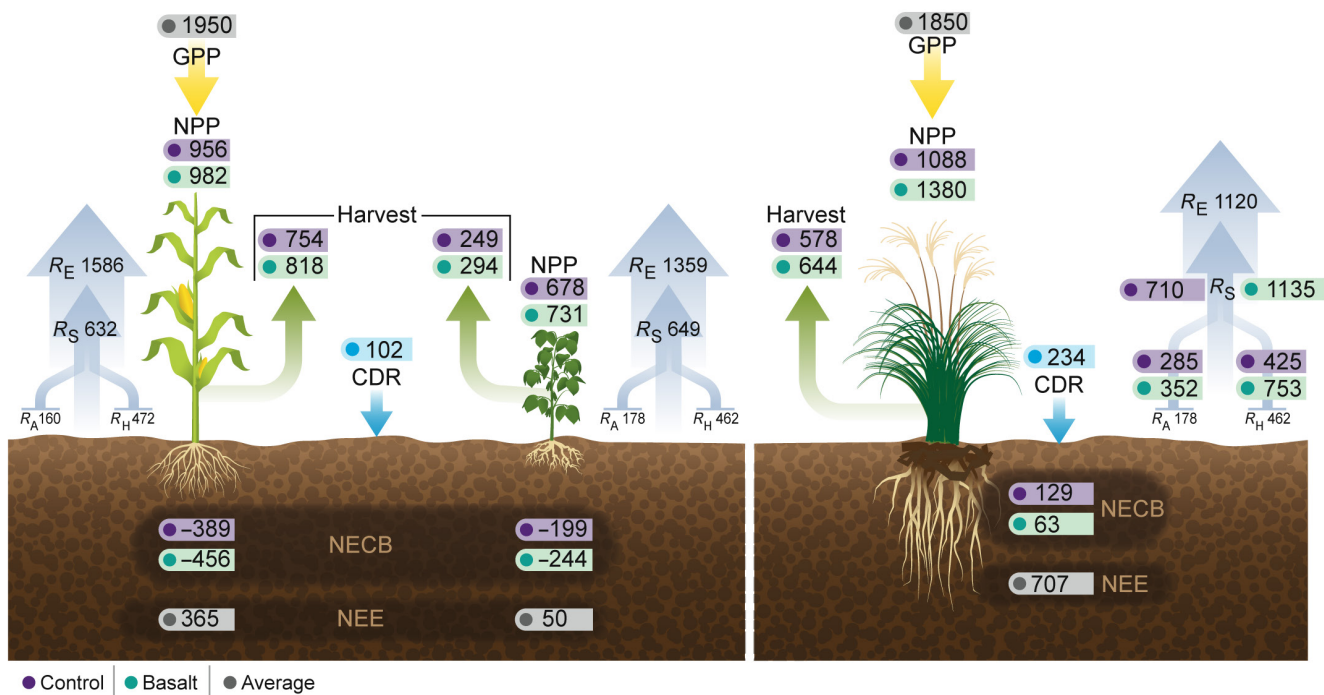


FIGURE 5 Partial carbon budgets for a maize [(a) left; average of 2017, 2018, 2020], soybean [(a) right; 2018], and miscanthus (b) (average of 2018, 2019, 2020) grown with or without basalt amendment. Where a difference in the underlying values used to create the carbon budget were significantly different, two numbers (lavender/control and green/basalt) are shown. If a statistical difference could not be detected in the underlying values, a single global average value is presented (gray boxes). All values are in units of $\text{g C m}^{-2} \text{ year}^{-1}$. GPP and NPP represent the transfer of carbon from the atmosphere to the land surface, and ecosystem respiration (R_E) represents the transfer of carbon from the land surface to the atmosphere. NEE and NECB are shown as positive or negative if carbon the net movement of carbon is to or away from the land surface, respectively. Soil respiration and its components, heterotrophic respiration and autotrophic respiration are indicated as R_S , R_H , and R_A , respectively. CDR (bright blue) represents carbon removal by enhanced weathering and is expressed as $\text{g C m}^{-2} \text{ year}^{-1}$. CDR, carbon dioxide removal; GPP, gross primary productivity; NECB, net ecosystem carbon balance; NEE, net ecosystem exchange; NPP, net primary productivity.

23%–42%. Although insufficient to offset carbon losses from these conventionally tilled row crops, this carbon removal strategy if applied to the 36 Mha each of maize and soybean planted in the US would sequester 179 t C year⁻¹. The additional 234 g C m⁻² year⁻¹ sequestered by EW added to the already positive NECB of miscanthus (Figure 5), generating a strong carbon sink for this cropping system. The US Midwest is a net source of CO₂ to the atmosphere with approximately 40% of the maize produced converted to fuel ethanol (Davis et al., 2011). Model predictions indicate that replacing maize ethanol with miscanthus would switch the Midwest from a source to a carbon sink, and switching to cellulosic biofuels like miscanthus nationally could reduce emissions by more than 12% (Hudiburg et al., 2016). The addition of basalt could greatly decrease the already low carbon intensity of miscanthus further increasing its value as a bioenergy crop. It is important to note, that unlike carbon stored as soil organic matter which is potentially oxidized and released back to the atmosphere with changing management practices, EW represents a pump of inorganic carbon from the atmosphere, through soil to groundwater and ultimately to the ocean, and can be viewed as permanent storage.

Agricultural lands are the testing ground for EW because they are widespread, provide access to equipment, and their necessity for

food production increases the likelihood the lands will stay in agriculture. Grain from the maize/soybean rotation is a food source for humans and livestock, and maize is the dominant bioethanol feedstock in the United States, occupying 28 Mha of farmland (Sands et al., 2017). The widespread production of the maize/soybean rotation makes it an enticing EW cropping system, as the effectiveness of EW at shifting the global carbon balance will demand careful accounting of the carbon costs of production and transport of the weathering material to the field. The ubiquitous nature of maize/soybean production creates opportunities to source the EW parent material close to where it will be applied, reducing transportation costs. Miscanthus, because of its large root system and reduced need for tillage, stores vast amounts of carbon as soil organic carbon and EW in this crop almost doubles this amount of carbon storage, greatly increasing the potential of this cellulosic bioenergy crop to offset carbon emissions from fuel.

4 | CONCLUSIONS

Intensive management caused the maize/soybean cropping system to be a source of carbon to the atmosphere with strongly negative

NECB. Basalt additions, by pumping inorganic carbon from the atmosphere to ground water, effectively offset 42% of carbon emissions from maize/soybean, and when paired with conservation tillage or cover cropping could turn this cropping system into a net carbon sink. In perennial miscanthus, the prolific root system and no-till management practices resulted in a strongly positive NECB, and EW further increased the sink strength of this cropping system. The primary value of bioenergy crops is the displacement of fossil fuels; the added benefit of increasing soil organic carbon and pumping inorganic carbon to ground water by EW greatly increases the climate benefits of these crops. The monitoring of accumulated REEs alongside the depletion of base cations in the topsoil provided a measurement of basalt applied as well as in-situ determined weathering rates and CDR potentials. As EW is explored in new ecosystems, the ability to accurately calculate time-dependent weathering rates and CDR potentials will become a critical component in optimizing carbon sequestration. In addition to the co-benefits of basalt application, including increased soil fertility and pH, as well as greater yields, this CDR strategy appears to be effective on rich Midwestern US soils.

ACKNOWLEDGMENTS

This research was supported by the Leverhulme Trust, Leverhulme Research Centre grant RC-2015-029 and by the DOE Center for Advanced Bioenergy and Bioproducts Innovation (U.S. Department of Energy, Office of Science, Office of Biological and Environmental Research under Award Number DE-SC0018420). We thank Tim Mies for logistical assistance and Adam Davis and the Department of Crop Sciences at the University of Illinois for providing land for this research.

CONFLICT OF INTEREST STATEMENT

Elliot Chang, Alison Marklein, and Adam Wolf acknowledge employment at Eion Corp, a Public Benefit Corporation in the United States, scaling terrestrial EW practices in agricultural systems. David J. Beerling has a minority equity stake in Future Forest/Undo. The involved authors contributed to this research program as industry collaborators with the Leverhulme Center for Climate Change Mitigation. Other authors have no conflicts to declare.

DATA AVAILABILITY STATEMENT

The data that support the findings of this study are available in the Illinois Data Bank (databank.illinois.edu) at the University of Illinois at https://doi.org/10.13012/B2IDB-1917166_V1. Historic eddy covariance flux data for this site are available via AmeriFlux (ameriflux.lbl.gov) at <https://doi.org/10.17190/AMF/1846665> and <https://doi.org/10.17190/AMF/1846664>.

ORCID

Adam von Haden  <https://orcid.org/0000-0003-3817-9352>
 Carl J. Bernacchi  <https://orcid.org/0000-0002-2397-425X>
 David J. Beerling  <https://orcid.org/0000-0003-1869-4314>
 Evan H. DeLucia  <https://orcid.org/0000-0003-3400-6286>

REFERENCES

- Alcántara, V., Don, A., Well, R., & Nieder, R. (2016). Deep ploughing increases agricultural soil organic matter stocks. *Global Change Biology*, 22, 2939–2956. <https://doi.org/10.1111/gcb.13289>
- Anda, M., Shamshuddin, J., & Fauziah, C. I. (2015). Improving chemical properties of a highly weathered soil using finely ground basalt rocks. *Catena*, 124, 147–161. <https://doi.org/10.1016/j.catena.2014.09.012>
- Anderson-Teixeira, K. J., Davis, S. C., Masters, M. D., & DeLucia, E. H. (2009). Changes in soil organic carbon under biofuel crops. *GCB Bioenergy*, 1, 75–96.
- Anderson-Teixeira, K. J., Masters, M. D., Black, C. K., Zeri, M., Hussain, M. Z., Bernacchi, C. J., & DeLucia, E. H. (2013). Altered belowground carbon cycling following land-use change to perennial bioenergy crops. *Ecosystems*, 16, 508–520. <https://doi.org/10.1007/s10021-012-9628-x>
- Angel, J. (2010). *Official 1981–2010 climate normals for Champaign Willard AP*. Illinois State Water Survey, Prairie Research Institute, University of Illinois.
- Baldocchi, D. D. (2003). Assessing the eddy covariance technique for evaluating carbon dioxide exchange of ecosystems: Past, present and future. *Global Change Biology*, 9, 479–492.
- Beerling, D. J., Kantzas, E. P., Lomas, M. R., Wade, P., Eufrasio, R. M., Renforth, P., Sarkar, B., Andrews, M. G., James, R. H., Pearce, C. R., Mercure, J. F., Pollitt, H., Holden, P. B., Edwards, N. R., Khanna, M., Koh, L., Quegan, S., Pidgeon, N. F., Janssens, I. A., ... Banwart, S. A. (2020). Potential for large-scale CO₂ removal via enhanced rock weathering with croplands. *Nature*, 583, 242–248. <https://doi.org/10.1038/s41586-020-2448-9>
- Bernacchi, C. J., Blakely, B., Moore, C., & Pederson, T. (2022). AmeriFlux BASE US-UIC University of Illinois maize-soy, ver. 1-5, AmeriFlux AMP. [Data set]. <https://doi.org/10.17190/AMF/1846665>
- Black, C. K., Davis, S. C., Hudiburg, T. W., Bernacchi, C. J., & DeLucia, E. H. (2016). Elevated CO₂ and temperature increase soil C losses from a soybean-maize ecosystem. *Global Change Biology*, 23, 435–445. <https://doi.org/10.1111/gcb.13378>
- Black, C. K., Masters, M. D., LeBauer, D. S., Anderson-Teixera, K. J., & DeLucia, E. H. (2017). Root volume distribution of maturing perennial grasses revealed by correcting for minirhizotron surface effects. *Plant and Soil*, 419, 391–404. <https://doi.org/10.1007/s11104-017-3333-7>
- Blakely, B., Moore, C., Bernacchi, C. J., & Pederson, T. (2022). AmeriFlux BASE US-UIC University of Illinois miscanthus, ver. 1-5, AmeriFlux AMP. [Data set]. <https://doi.org/10.17190/AMF/1846664>
- Blanc-Betes, E., Kantola, I. B., Gomez-Casanovas, N., Hartman, M. D., Parton, W. J., Lewis, A. L., Beerling, D. J., & DeLucia, E. H. (2020). In silico assessment of the potential of basalt amendments to reduce N₂O emissions from bioenergy crops. *GCB Bioenergy*, 12, 941–954.
- Chang, E., Brewer, W. A., Park, M. D., Jiao, Y., & Lammers, N. L. (2021). Selective biosorption of valuable rare earth elements among co-occurring lanthanides. *Environmental Engineering Science*, 38, 154–164. <https://doi.org/10.1089/ees.2020.0291>
- Chapin, F. S., Woodwell, G. M., Randerson, J. T., Rastetter, E. B., Lovett, G. M., Baldocchi, D. D., Clark, D. A., Harmon, M. E., Schimel, D. S., Valentini, R., Wirth, C., Aber, J. D., Cole, J. J., Goulden, M. L., Harden, J. W., Heimann, M., Howarth, R. W., Matson, P. A., McGuire, A. D., ... Schulze, E. D. (2006). Reconciling carbon-cycle concepts, terminology, and methods. *Ecosystems*, 9, 1041–1050. <https://doi.org/10.1007/s10021-005-0105-7>
- Chen, H., Zhang, C., Guo, H., Hu, Y., He, Y., & Jiang, D. (2018). Overexpression of *Miscanthus sacchariflorus* yellow stripe-like transporter MsYSL1 enhances resistance of *Arabidopsis* by cadmium by mediating metal ion reallocation. *Plant Growth Regulation*, 85, 1001–1111.
- Curtin, D., Campbell, C. A., & Jalil, A. (1998). Effects of acidity on mineralization: pH-dependence of organic matter mineralization in weakly acidic soils. *Soil Biology and Biochemistry*, 30, 57–64.

- Davis, S. C., Parton, W. J., Del Grosso, S. J., Keough, C., Marx, E., Adler, P. R., & DeLucia, E. H. (2011). Impact of second-generation biofuel agriculture on greenhouse-gas emissions in the corn-growing regions of the US. *Frontiers in Ecology and the Environment*, 10, 69–74. <https://doi.org/10.1890/110003>
- Davis, S. C., Parton, W. J., Dohleman, F. G., Smith, C. M., Del Grosso, S., Kent, A. D., & DeLucia, E. H. (2010). Comparative biogeochemical cycles of bioenergy crops reveal nitrogen-fixation and low greenhouse gas emissions in a *Miscanthus × giganteus* agro-ecosystem. *Ecosystems*, 13, 144–156.
- DeLucia, E. H., Chen, S., Guan, K., Peng, B., Li, Y., Gomez-Casanovas, N., Kantola, I. B., Bernacchi, C. J., Huang, Y., Long, S. P., & Ort, D. R. (2019). Are we approaching a water ceiling to maize yields in the United States? *Ecosphere*, 10(6), e02773.
- Dohleman, F. G., Heaton, E. A., Arundale, R. A., & Long, S. P. (2012). Seasonal dynamics of above- and below-ground biomass and nitrogen partitioning in *Miscanthus giganteus* and *Panicum virgatum* across three growing seasons. *Global Change Biology Bioenergy*, 4, 534–544.
- Dohleman, F. G., & Long, S. P. (2009). More productive than maize in the Midwest: How does miscanthus do it? *Plant Physiology*, 150, 2104–2115.
- Epiphov, D. Z., Batterman, S. A., Hedin, L. O., Leake, J. R., Smith, L. M., & Beerling, D. J. (2017). N₂-fixing tropical legume evolution: A contributor to enhanced weathering through the Cenozoic? *Proceedings of the Royal Society B: Biological Sciences*, 284(1860), 20170370.
- Epiphov, D. Z., Saltonstall, K., Batterman, S. A., Hedin, L. O., Hall, J. S., van Breugel, M., Leake, J. R., & Beerling, D. J. (2021). Legume-microbiome interactions unlock mineral nutrients in regrowing tropical forests. *Proceedings of the National Academy of Sciences of the United States of America*, 118(11), e2022241118.
- Fargione, J. E., Bassett, S., Boucher, T., Bridgeman, S. D., Conant, R. T., Cook-Patton, S. C., Ellis, P. W., Falcucci, A., Fourqurean, J. W., Gopalakrishna, T., Gu, H., Henderson, B., Hurteau, M. D., Kroeger, K. D., Megonigal, J. P., Miteva, D. A., Richardson, C. J., Sanderman, J., Schoch, D., ... Griscom, B. W. (2018). Natural climate solutions for the United States. *Science Advances*, 4, eaat1869. <https://doi.org/10.1126/sciadv.aat1869>
- Fawzy, S., Osman, A. I., Mehta, N., Moran, D., Al-Muhtaseb, A. H., & Rooney, D. W. (2022). Atmospheric carbon removal via industrial biochar systems: A techno-economic-environmental study. *Journal of Cleaner Production*, 371, 133660. <https://doi.org/10.1016/j.jclepro.2022.133660>
- Gill, R. A., & Jackson, R. B. (2000). Global patterns of root turnover for terrestrial ecosystems. *New Phytologist*, 147, 13–31.
- Gillman, G. P., Burkett, D. C., & Coventry, R. J. (2002). Amending highly weathered soils with finely ground basalt rock. *Applied Geochemistry*, 17, 987–1001.
- Gomez-Casanovas, N., Anderson-Teixeira, K. J., Zeri, M., Bernacchi, C. J., & DeLucia, E. H. (2013). Gap filling strategies and error in estimating annual soil respiration. *Global Change Biology*, 19, 1941–1952. <https://doi.org/10.1111/gcb.12127>
- Hartmann, J., West, A. J., Renforth, P., Köhler, P., De La Rocha, C. L., Wolf-Gladrow, D. A., Dürr, H. H., & Scheffran, J. (2013). Enhanced chemical weathering as a geoengineering strategy to reduce atmospheric carbon dioxide, supply nutrients, and mitigate ocean acidification. *Reviews of Geophysics*, 51, 113–149. <https://doi.org/10.1002/rog.20004>
- Hasegawa, T., Fujimori, S., Frank, S., Humpenoder, F., Bertram, C., Despres, J., Drouet, L., Emmerling, J., Gusti, M., Harmsen, M., Keramida, K., Ochi, Y., Oshiro, K., Rochedo, P., van Ruijven, B., Cabardos, A.-M., Deppermann, A., Fosse, F., Havlik, P., ... Riahi, K. (2021). Land-based implications of early climate actions without global net-negative emissions. *Nature Sustainability*, 4, 1052–1059.
- Hudiburg, T. W., Davis, S. C., Parton, W., & DeLucia, E. H. (2014). Bioenergy crop greenhouse gas mitigation potential under a range of management practices. *Global Change Biology Bioenergy*, 7, 366–374. <https://doi.org/10.1111/gccb.12152>
- Hudiburg, T. W., Wang, W. W., Khanna, M., Long, S. P., Dwivedi, P., Parton, W. J., Hartman, M., & DeLucia, E. H. (2016). Impacts of a 32-billion-gallon bioenergy landscape on land fossil fuel use in the US. *Nature Energy*, 1, 15005. <https://doi.org/10.1038/nenergy.2015.5>
- Isaac, P., Cleverly, J., McHugh, I., van Gorsel, E., Ewenz, C., & Beringer, J. (2017). OzFlux Data: Network integration from collection to curation. *Biogeosciences*, 14, 1–41. <https://doi.org/10.5194/bg-14-2903-2017>
- Isson, T., Planavsky, N., Coogan, L., Stewart, E., Ague, J., Bolton, E., Zhang, S., McKenzie, N. R., & Kump, L. R. (2020). Evolution of the global carbon cycle and climate regulation on earth. *Global Biogeochemical Cycles*, 34(2), e2018GB006061.
- Jariwala, J., Haque, F., Vanderburgt, S., Santos, R. M., & Chiang, Y. W. (2022). Mineral-soil-plant-nutrient synergisms of enhanced weathering for agriculture: Short-term investigations using fast-weathering wollastonite skarn. *Frontiers in Plant Science*, 13, 929457. <https://doi.org/10.3389/fpls.2022.929457>
- Joo, E., Zaman Hussain, M., Zeri, M., Masters, M. D., Miller, J. N., Gomez-Casanovas, N., DeLucia, E. H., & Bernacchi, C. J. (2016). The influence of drought and heat stress on long-term carbon fluxes of bioenergy crops grown in the Midwestern USA. *Plant, Cell, and Environment*, 39, 1928–1940.
- Joo, E., Zeri, M., Hussain, M. Z., DeLucia, E. H., & Bernacchi, C. J. (2017). Enhanced evapotranspiration was observed during extreme drought from miscanthus, opposite of other crops. *Global Change Biology Bioenergy*, 9, 1306–1319.
- Kantola, I. B., Blanc-Betes, E., Masters, M. D., Chang, E., Marklein, A., Moore, C. E., von Haden, A., Bernacchi, C. J., Wolf, A., Epiphov, D. Z., Beerling, D. J., & DeLucia, E. H. (2023). Data from: Improved net carbon budgets in the US Midwest through direct measured impacts of enhanced weathering [Data set]. Illinois Data Bank, University of Illinois at Urbana-Champaign. https://doi.org/10.13012/B2IDB-1917166_V1
- Kantola, I. B., Masters, M. D., Beerling, D. J., Long, S. P., & DeLucia, E. H. (2017). Potential of global croplands and bioenergy crops for climate change mitigation through deployment of enhanced weathering. *Biology Letters*, 13, 20160714.
- Kantola, I. B., Masters, M. D., Blanc-Betes, E., Gomez-Casanovas, N., & DeLucia, E. H. (2022). Long-term yields in annual and perennial bio-energy crops in the Midwestern United States. *Global Change Biology Bioenergy*, 14, 694–706. <https://doi.org/10.1111/gccb.12940>
- Kelland, M. E., Wade, P. W., Lewis, A. L., Taylor, L. L., Sarkar, B., Andrews, M. G., Lomas, M. R., Cotton, T. E. A., Kemp, S. J., James, R. H., Pearce, C. R., Hartley, S. E., Hodson, M. E., Leake, J. R., Banwart, S. A., & Beerling, D. J. (2020). Increased yield and CO₂ sequestration potential with the C₄ cereal *Sorghum bicolor* cultivated in basaltic rock dust-amended agricultural soil. *Global Change Biology*, 26, 3658–3676. <https://doi.org/10.1111/gcb.15089>
- Kohler, P., Hartmann, J., & Wolf-Gladrow, D. A. (2010). Geoengineering potential of artificially enhanced silicate weathering of olivine. *Proceedings of the National Academy of Sciences of the United States of America*, 107, 20228–20233.
- Kumari, N., & Mohan, C. (2021). Basics of clay minerals and their characteristic properties. In G. M. Do Nascimento (Ed.), *Clay and clay minerals*. IntechOpen. <https://doi.org/10.5772/intechopen.97672>
- Kuzyakov, Y. (2006). Sources of CO₂ efflux from soil and review of partitioning methods. *Soil Biology and Biochemistry*, 38, 425–448.
- Larkin, C. S., Andrews, M. G., Pearce, C. R., Yeong, K. L., Beerling, D. J., Bellamy, J., Benedick, S., Freckleton, R. P., Goring-Harford, H., Sadekar, S., & James, R. H. (2022). Quantification of CO₂ removal in a large-scale enhanced weathering field trial on an oil palm plantation in Sabah, Malaysia. *Frontiers in Climate*, 4, 959229. <https://doi.org/10.3389/fclim.2022.959229>

- Levy, R. (1980). Sources of soluble calcium and magnesium and their effects on sodium adsorption ratios of solutions in two soils of Israel. *Geoderma*, 23, 113–123. [https://doi.org/10.1016/0016-7061\(80\)90014-2](https://doi.org/10.1016/0016-7061(80)90014-2)
- Lewis, A. L., Sarkar, B., Wade, P., Kemp, S. J., Hodson, M. E., Taylor, L. L., Yeong, K. L., Davies, K., Nelson, P. N., Bird, M. I., Kantola, I. B., Masters, M. D., DeLucia, E., Leake, J. R., Banward, S. A., & Beerling, D. J. (2021). Effects of mineralogy, chemistry and physical properties of basalt on carbon capture potential and plant-nutrient element release via enhanced weathering. *Applied Geochemistry*, 132, 10502.
- Liang, T., Song, W., Wang, L., Kleinman, P. J. A., & Cao, H. (2010). Interactions between exogenous rare earth elements and phosphorus leaching in packed soil columns. *Pedosphere*, 20, 616–622. [https://doi.org/10.1016/S1002-0160\(10\)60051-3](https://doi.org/10.1016/S1002-0160(10)60051-3)
- Liu, P., Tian, J., Zhou, P., Yang, M., & Shi, H. (2004). Stable rare earth element tracers to evaluate soil erosion. *Soil and Tillage Research*, 76, 147–155. <https://doi.org/10.1016/j.still.2003.09.005>
- Lloyd, T., & Taylor, J. A. (1994). On the temperature-dependence of soil respiration. *Functional Ecology*, 9, 315–323.
- Lobell, D. B., Roberts, M. J., Schlenker, W., Braun, N., Little, B. B., Rejesus, R. M., & Hammer, G. L. (2014). Greater sensitivity to drought accompanies maize yield increase in the US Midwest. *Science*, 344, 516–519.
- Migaszewski, Z. M., & Galuszka, A. (2015). The characteristics, occurrence, and geochemical behavior of rare earth elements in the environment: A review. *Critical Reviews in Environmental Science and Technology*, 45, 429–471.
- Minx, J. C., Lamb, W. F., Callaghan, M. W., Bormann, L., & Fuss, S. (2017). Fast growing research on negative emissions. *Environmental Research Letters*, 12, 035007.
- Moore, C. E., Berardi, D. M., Blanc-Betés, E., Dracup, E. C., Egenriether, S., Gomez-Casanovas, N., Hartman, M. D., Hudiburg, T., Kantola, I., Masters, M. D., Parton, W. J., Van Allen, R., Haden, A. C., Yang, W. H., DeLucia, E. H., & Bernacchi, C. J. (2020). The carbon and nitrogen cycle impacts of reverting perennial bioenergy switchgrass to an annual maize crop rotation. *Global Change Biology Bioenergy*, 12, 941–954. <https://doi.org/10.1111/gcbb.12743>
- Moore, C. E., Gibson, C. D., Miao, G., Dracup, E. C., Gomez-Casanovas, N., Masters, M. D., Miller, J., Von Haden, A. C., Meyers, T., DeLucia, E. H., & Bernacchi, C. J. (2022). Substantial carbon loss respired from corn-soybean agroecosystems highlights the importance of careful management as we adapt to changing climate. *Environmental Research Letters*, 17, 054029.
- Moosdorf, N., Renforth, P., & Hartman, J. (2014). Carbon dioxide efficiency of terrestrial enhanced weathering. *Environmental Science and Technology*, 48, 4809–4816.
- Nelson, A. J., Lichiheb, N., Koloutsou-Vakakis, S., Rood, M. J., Heuer, M., Myles, L. T., Joo, E., Miller, J., & Bernacchi, C. (2019). Ammonia flux measurements above a corn canopy using relaxed eddy accumulation and a flux gradient system. *Agricultural and Forest Meteorology*, 264, 104–113. <https://doi.org/10.1016/j.agrforestmet.2018.10.003>
- Ozaki, T., Suzuki, Y., Nankawa, T., Yoshida, T., Ohnuki, T., Kimura, T., & Francisc, A. J. (2006). Interactions of rare earth elements with bacteria and organic ligands. *Journal of Alloys and Compounds*, 408–412, 1334–1338. <https://doi.org/10.1016/j.jallcom.2005.04.142>
- Papale, D., Reichstein, M., Aubinet, M., Canfora, E., Bernhofer, C., Kutsch, W., Longdoz, B., Rambal, S., Valentini, R., Vesala, T., & Yakir, D. (2006). Towards a standardized processing of net ecosystem exchange measured with eddy covariance technique: Algorithms and uncertainty estimation. *Biogeosciences*, 3, 571–583. <https://doi.org/10.5194/bg-3-571-2006>
- Renforth, P. (2018). The negative emission potential of alkaline materials. *Nature Communications*, 10, 1401. <https://doi.org/10.1038/s41467-019-09475-5>
- Renforth, P., & Henderson, G. (2017). Assessing ocean alkalinity for carbon sequestration. *Reviews of Geophysics*, 55, 636–674. <https://doi.org/10.1002/2016RG000533>
- Renforth, P., Washbourne, C. L., Taylder, J., & Manning, D. A. C. (2011). Silicate production and availability for mineral carbonation. *Environmental Science & Technology*, 2011, 2035–2041. <https://doi.org/10.1021/es103241w>
- Rogelj, J., Shindell, D., Jiang, K., Fiftia, S. M., Forster, P., Ginzburg, V., Handa, C., Khisigi, H., Kobayashi, S., Kriegler, E., Mundaca, L., Seferian, R., & Vilarino, M. (2018). Mitigation pathways compatible with 1.5°C in the context of sustainable development. In *Global warming of 1.5°C*. An IPCC special report on the impact of global warming of 1.5°C above pre-industrial levels and related global greenhouse emission pathways, in the context of strengthening the global response to the threat of climate change. Intergovernmental Panel on Climate Change. https://www.ipcc.ch/site/assets/uploads/sites/2/2019/05/SR15_Chapter2_Low_res.pdf
- Sands, R. D., Malcolm, S. A., Suttles, S. A., & Marshall, E. (2017). *Dedicated energy crops and competition for agricultural lands*. ERR-223. US Department of Agriculture, Economic Research Service, January 2017.
- Schnitkey, G., Zulauf, C., Swanson, K., & Paulson, N. (2021). Recent state soybean and corn yields in Illinois. *Farmdoc Daily*, 11, 68. Department of Agricultural and Consumer Economics, University of Illinois at Urbana-Champaign, April 27, 2021.
- Schuling, R. D., & Krijgsman, P. (2006). Enhanced weathering: An effective and cheap tool to sequester CO₂. *Climatic Change*, 74, 349–354. <https://doi.org/10.1007/s10584-005-3485-y>
- Shibata, S., Tanaka, T., & Yamamoto, K. (2006). Crystal structure control of the dissolution of rare earth elements in water-mineral interactions. *Geochemical Journal*, 40, 437–446. <https://doi.org/10.2343/geochem.40.437>
- Silver, W. E., Vergara, S. E., & Mayer, A. (2018). Carbon sequestration and greenhouse gas mitigation potential of composting and soil amendments on California's rangelands. California's Fourth Climate Change Assessment, California Natural Resources Agency. Publication number CCCA4-CNRA2018-002.
- Somerville, C., Yongs, H., Taylor, C., Davis, S. C., & Long, S. P. (2010). Feedstocks for lignocellulosic biofuels. *Science*, 329, 790–792.
- Suyker, A. E., & Verma, S. B. (2012). Gross primary production and ecosystem respiration of irrigated and rainfed maize-soybean cropping systems of 8 years. *Agricultural and Forest Meteorology*, 165, 12–24.
- Takahashi, Y., Kondo, K., Miyaji, A., Watanabe, Y., Fan, Q., Honma, T., & Tanaka, K. (2014). Recovery and separation of rare earth elements using salmon milt. *PLoS One*, 9, e114858. <https://doi.org/10.1371/journal.pone.0114858>
- Tang, J., & Johannesson, K. H. (2010). Ligand extraction of rare earth elements from aquifer sediments: Implications for rare earth element complexation with organic matter in natural waters. *Geochimica et Cosmochimica Acta*, 74, 6690–6705. <https://doi.org/10.1016/j.gca.2010.08.028>
- Taylor, L. L., Driscoll, C. T., Groffman, P. M., Rau, G. H., Blum, J. D., & Beerling, D. J. (2021). Increased carbon capture by silicate-treated forested watershed affected by acid deposition. *Biogeosciences*, 18, 169–188.
- Taylor, L. L., Quirk, J., Thorley, R. M. S., Kharecha, A., Hansen, J., Ridwell, A., Lomas, M. R., Banwart, S. A., & Beerling, D. J. (2016). Enhanced weathering strategies for stabilizing climate and averting ocean acidification. *Nature Climate Change*, 6, 402–408.
- United States Department of Agriculture, Natural Resources Conservation Service. (2022). Web soil survey for Champaign County, IL. <https://www.nrcs.usda.gov/resources/data-and-reports/web-soil-survey>
- United States Environmental Protection Agency. (2023). Global greenhouse gas emissions data. <https://www.epa.gov/ghgemissions/global-greenhouse-gas-emissions-data>
- Verma, S. B., Dobermann, A., Cassman, K. G., Walters, D. T., Knopps, J. M., Arkebauer, T. J., Suyker, A. E., Burba, G. G., Amos, B., Yang, H. S., Ginting, D., Hubbard, K. G., Gitelson, A. A., & Walter-Shea, E. A. (2005). Annual carbon dioxide exchange in irrigated and rainfed

- maize-based agroecosystems. *Agricultural and Forest Meteorology*, 131, 77–96.
- Vienne, A., Poblador, S., Portillo-Estrada, M., Hartmann, J., Ijehon, S., Wade, P., & Vicca, S. (2022). Enhanced weathering using basalt rock powder: Carbon sequestration, co-benefits and risks in a mesocosm study with *Solanum tuberosum*. *Frontiers in Climatology*, 4, 869456. <https://doi.org/10.3389/fclim.2022.869456>
- Walker, J. C., Hays, P., & Kasting, J. F. (1981). A negative feedback mechanism for the long-term stabilization of Earth's surface temperature. *Journal of Geophysical Research*, 86(C10), 9776–9782.
- Wildova, R., Wild, J., & Herben, T. (2007). Fine-scale dynamics of rhizomes in a grassland community. *Ecography*, 30, 264–276.
- Xiao, Y., Huang, L., Long, Z., Feng, Z., & Wang, L. (2016). Adsorption ability of rare earth elements on clay minerals and its practical performance. *Journal of Rare Earths*, 34, 543–548. [https://doi.org/10.1016/S1002-0721\(16\)60060-1](https://doi.org/10.1016/S1002-0721(16)60060-1)
- Zeri, M., Anderston-Teixeira, K., Hickman, G., Masters, M., DeLucia, E., & Bernacchi, C. J. (2011). Carbon exchange by establishing biofuel crops in Central Illinois. *Agriculture Ecosystems and Environment*, 144, 319–329.
- Zhang, X., Lark, T. J., Clark, C. M., Yuan, Y., & LeDuc, S. D. (2021). Grassland-to-cropland conversion increased soil, nutrient, and carbon losses in

the US Midwest between 2008 and 2016. *Environmental Research Letters*, 16, 054018. <https://doi.org/10.1088/1748-9326/abecbe>

SUPPORTING INFORMATION

Additional supporting information can be found online in the Supporting Information section at the end of this article.

How to cite this article: Kantola, I. B., Blanc-Betes, E., Masters, M. D., Chang, E., Marklein, A., Moore, C. E., von Haden, A., Bernacchi, C. J., Wolf, A., Epiphov, D. Z., Beerling, D. J., & DeLucia, E. H. (2023). Improved net carbon budgets in the US Midwest through direct measured impacts of enhanced weathering. *Global Change Biology*, 29, 7012–7028. <https://doi.org/10.1111/gcb.16903>